Redox regulation of MAPK phosphatase 1 controls monocyte migration and macrophage recruitment

Hong Seok Kim[a], Sarah L. Ullevig[b], Debora Zamora[a], Chi Fung Lee[b], and Reto Asmis[a,b,1]

Departments of [a]Clinical Laboratory Sciences and [b]Biochemistry, University of Texas Health Science Center at San Antonio, San Antonio, TX 78229-3904

Edited by Michael A. Gimbrone, Brigham and Woman's Hospital, Harvard Medical School, Boston, MA, and approved August 27, 2012 (received for review July 25, 2012)

Monocytic adhesion and chemotaxis are regulated by MAPK pathways, which in turn are controlled by redox-sensitive MAPK phosphatases (MKPs). We recently reported that metabolic disorders prime monocytes for enhanced recruitment into vascular lesions by increasing monocytes' responsiveness to chemoattractants. However, the molecular details of this proatherogenic mechanism were not known. Here we show that monocyte priming results in the *S*-glutathionylation and subsequent inactivation and degradation of MKP-1. Chronic exposure of human THP-1 monocytes to diabetic conditions resulted in the loss of MKP-1 protein levels, the hyperactivation of ERK and p38 in response to monocyte chemoattractant protein-1 (MCP-1), and increased monocyte adhesion and chemotaxis. Knockdown of MKP-1 mimicked the priming effects of metabolic stress, whereas MKP-1 overexpression blunted both MAPK activation and monocyte adhesion and migration induced by MCP-1. Metabolic stress promoted the *S*-glutathionylation of MKP-1, targeting MKP-1 for proteasomal degradation. Preventing MKP-1 *S*-glutathionylation in metabolically stressed monocytes by overexpressing glutaredoxin 1 protected MKP-1 from degradation and normalized monocyte adhesion and chemotaxis in response to MCP-1. Blood monocytes isolated from diabetic mice showed a 55% reduction in MKP-1 activity compared with nondiabetic mice. Hematopoietic MKP-1 deficiency in atherosclerosis-prone mice mimicked monocyte priming and dysfunction associated with metabolic disorders, increased monocyte chemotaxis in vivo, and accelerated atherosclerotic lesion formation. In conclusion, we identified MKP-1 as a central redox-sensitive regulator of monocyte adhesion and migration and showed that the loss of MKP-1 activity is a critical step in monocyte priming and the metabolic stress-induced conversion of blood monocytes into a proatherogenic phenotype.

inflammation | cell adhesion | cell migration | metabolic diseases

Metabolic disorders such as obesity and diabetes are associated with a state of chronic, low-grade inflammation (1, 2), which appears to contribute to the development of micro- and macrovascular complications such as atherosclerosis, nephropathy, and retinopathy (3–5). The cellular and molecular mechanisms involved in chronic inflammation associated with metabolic disorders are not yet fully understood, but the recruitment of blood monocytes to sites of vascular injury appears to play a central and rate-limiting role in all these complications. Metabolic disorders impact blood vessels at multiple levels, including lipid depositions, endothelial injury, and smooth muscle cell proliferation and migration, which individually or in concert initiate monocyte recruitment and promote vascular inflammation (6, 7). However, metabolic disorders also appear to affect blood monocytes directly. A number of studies reported that monocytes both in patients with metabolic disorders and in dyslipidemic or diabetic mice undergo phenotypical and functional changes that may contribute directly to the development and progression of chronic inflammatory vascular diseases (8–13).

Our recent studies explored this possibility, and we showed that metabolic stress primes monocytes for activation by chemoattractants, including monocyte chemoattractant protein-1 (MCP-1, also known as "CCL2," "SCYA2," and "MCAF"), a major chemoattractant involved in the recruitment of macrophages into atherosclerotic lesions (14–16), transforming these cells into a hypermigratory, proinflammatory phenotype (17, 18). In dyslipidemic and in diabetic mice the increased responsiveness of monocytes to chemokine-induced migration correlated with the level of intracellular thiol oxidative stress and was a strong predictor of both lesion size and macrophage content of atherosclerotic plaques (17, 18). Monocyte priming by metabolic stress is mediated by the induction of Nox4, an NADPH oxidase recently identified in monocytes and macrophages (19). We also showed that the increased production of Nox4-derived H_2O_2 targets reactive protein thiols and promotes protein *S*-glutathionylation, i.e., the formation of mixed disulfides between protein cysteine residues and glutathione (GSH). Overexpression of glutaredoxin 1 (Grx1), the enzyme that catalyzes the reduction of protein–GSH mixed disulfides, blocked protein *S*-glutathionylation induced by metabolic stress and protected monocytes from the hyperresponsiveness to chemokine-induced migration. However, the signaling pathways involved in monocyte priming and the signaling molecules regulated by *S*-glutathionylation remained unknown.

Monocyte transmigration into the vessel wall initiates atherogenesis, but this inflammatory process can continue throughout plaque development. Monocyte recruitment, which during the early stages of atherogenesis is driven primarily by MCP-1 (14–16), involves two major processes: monocyte adhesion and chemotaxis. Both processes are regulated by MAPK pathways. In THP-1 monocytes, ERK primarily regulates integrin activation and firm adhesion of monocytes, whereas chemotaxis is under the control of p38 (20, 21). Both p38 and ERK are counterregulated and inactivated by MAPK phosphatases (MKPs) (22, 23), suggesting that MKPs also may play an important role in monocyte migration and recruitment. Evidence from a number of studies suggests that both p38 and ERK pathways are redox sensitive. Reactive oxygen species (ROS) were reported to promote the activation of these MAPKs (24–28), whereas ROS scavengers appear to prevent MAPK activation (29). MKPs have the same catalytic cysteine residue as PTP-1B, a well-known site of *S*-glutathionylation and PTP-1B inactivation (30). In this study, we provide evidence that MKP-1, an MKP implicated in the migration of smooth muscle cells (31), is a central redox-sensitive regulator of monocyte adhesion and chemotaxis. Furthermore, we show that Nox4-derived H_2O_2 induced by metabolic stress targets and inactivates MKP-1 in monocytes. Moreover, we demonstrate that loss of MKP-1 activity induces monocyte priming and promotes accelerated trans-

Author contributions: H.S.K. and R.A. designed research; H.S.K., S.L.U., D.Z., C.F.L., and R.A. performed research; H.S.K., C.F.L., and R.A. contributed new reagents/analytic tools; H.S.K., S.L.U., D.Z., C.F.L., and R.A. analyzed data; and H.S.K. and R.A. wrote the paper.

The authors declare no conflict of interest.

This article is a PNAS Direct Submission.

[1]To whom correspondence should be addressed. Email: asmis@uthscsa.edu.

See Author Summary on page 16422 (volume 109, number 41).

This article contains supporting information online at www.pnas.org/lookup/suppl/doi:10.1073/pnas.1212596109/-/DCSupplemental.

migration and recruitment of metabolically stressed monocytes. Our data therefore support a redox-regulated mechanism that directly links oxidative stress associated with metabolic disorders to monocyte-dependent, chronic inflammatory diseases.

Results

Monocytes Primed by Metabolic Stress Display Accelerated Cell Adhesion and Chemotaxis in Response to MCP-1 and Hyperactivation of ERK and p38. To examine whether metabolic stress sensitizes or primes monocytes for MCP-1 activation, we preincubated monocytes with human LDL (100 μg/mL) plus high glucose (25 mM) for 24 h and examined cell adhesion and migration in response to MCP-1. Primed THP-1 monocytes showed a 2.4-fold acceleration of adhesion and a 1.8-fold increase in chemotaxis (Fig. 1 *A* and *B*). Metabolic stress also increased cell adhesion of primary human blood monocytes by 1.3-fold (Fig. 1*C*) and accelerated cell migration by 1.5-fold (Fig. 1*D*), suggesting that monocyte priming by metabolic stress may occur in patients with metabolic disorders. Monocyte adhesion is activated primarily via the ERK pathway, whereas p38 regulates monocyte chemotaxis (20, 21). To examine whether monocyte priming occurs at the level of ERK and p38 activation, we measured ERK and p38 phosphorylation in response to MCP-1 stimulation. As shown in Fig. 1 *E* and *F*, priming of THP-1 monocytes by metabolic stress resulted in the sustained hyperphosphorylation and hyperactivation of both ERK and p38 in response to MCP-1 stimulation. Interestingly, in contrast to ERK, p38 already was hyperactivated in primed cells before MCP-1 stimulation.

Inhibition of MKP-1 Activity Mimics Monocyte Priming by Metabolic Stress. ERK and p38 are counterregulated and inactivated by MKPs, a subgroup of dual-specificity phosphatases (23). Western blot analysis revealed that MKP-1 levels were decreased by 26% in monocytes exposed to metabolic stress (Fig. 2*A* and Fig. S1). Loss of MKP-1 protein in primed monocytes coincided with a 44% decrease in MKP-1 activity (Fig. 2*B*), suggesting that the partial inactivation of MKP-1 induced by metabolic stress may account for the hyperactivation of ERK and p38 in primed monocytes. We therefore used knockdown approaches to mimic the loss of MKP-1 activity by inactivation plus degradation and to explore whether reduced MKP-1 activity alone is sufficient to recapitulate monocytes priming by metabolic stress. RNAi-mediated knockdown of MKP-1 protein levels by 56% (Fig. 2*C*) accelerated MCP-1–induced adhesion of THP-1 monocytes by 1.5-fold (Fig. 2*D*) and increased monocyte chemotaxis by 1.4-fold (Fig. 2*E*). Similar to our findings in monocytes primed by metabolic stress, MCP-1 stimulation of MKP-1–deficient monocytes resulted in the sustained hyperactivation of both ERK and p38 (Fig. 2 *F* and *G*); again, p38, but not ERK, already was hyperactivated before MCP-1 stimulation.

Overexpression of MKP-1 Inhibits MCP-1–Induced Monocyte Adhesion and Chemotaxis. To explore further the functional roles of MKP-1 in monocyte adhesion and migration, we overexpressed Flag-

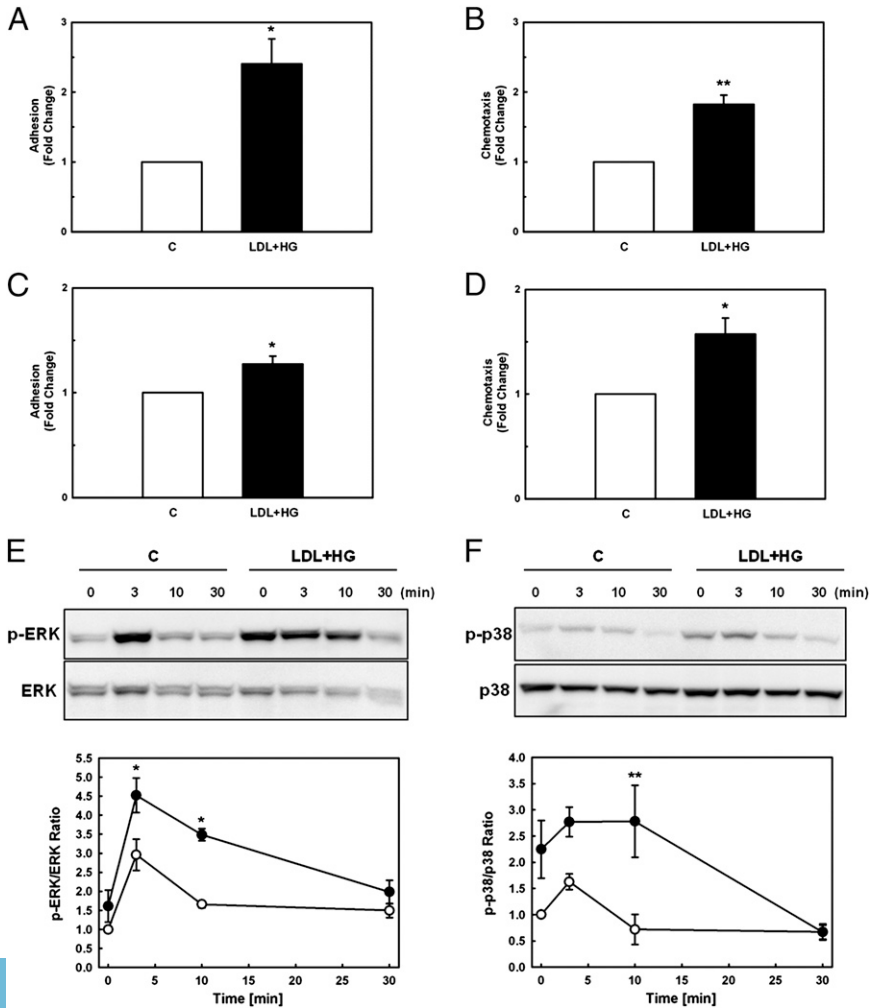

Fig. 1. Metabolic stress primes monocytes for accelerated cell adhesion and chemotaxis and hyperactivation of ERK and p38 in response to MCP-1. THP-1 monocytes were preincubated for 24 h with 100 μg/mL of LDL and 25 mM glucose (LDL+HG) or vehicle control (C). (*A*–*D*) Cell adhesion on fibronectin (*A*) or chemotaxis (*B*) was induced with 2 nM MCP-1 as described in *Materials and Methods*. Identical adhesion (*C*) and chemotaxis (*D*) assays were conducted with unprimed (C) and primed (LDL+HG) purified primary human blood monocytes. (*E* and *F*) (*Lower*) Activation of ERK (*E*) and p38 (*F*) by MCP-1 was analyzed in vehicle-treated (open circles) and metabolically primed THP-1 monocytes (LDL+HG; closed circles). MAPK activation was assessed by Western blot analysis at the indicated times as phosphorylation of ERK (*E*) and p38 (*F*). (*Upper*) Representative Western blots are shown. Results are presented as means ± SE of three to five independent experiments. $^{*}P < 0.05$; $^{**}P < 0.01$.

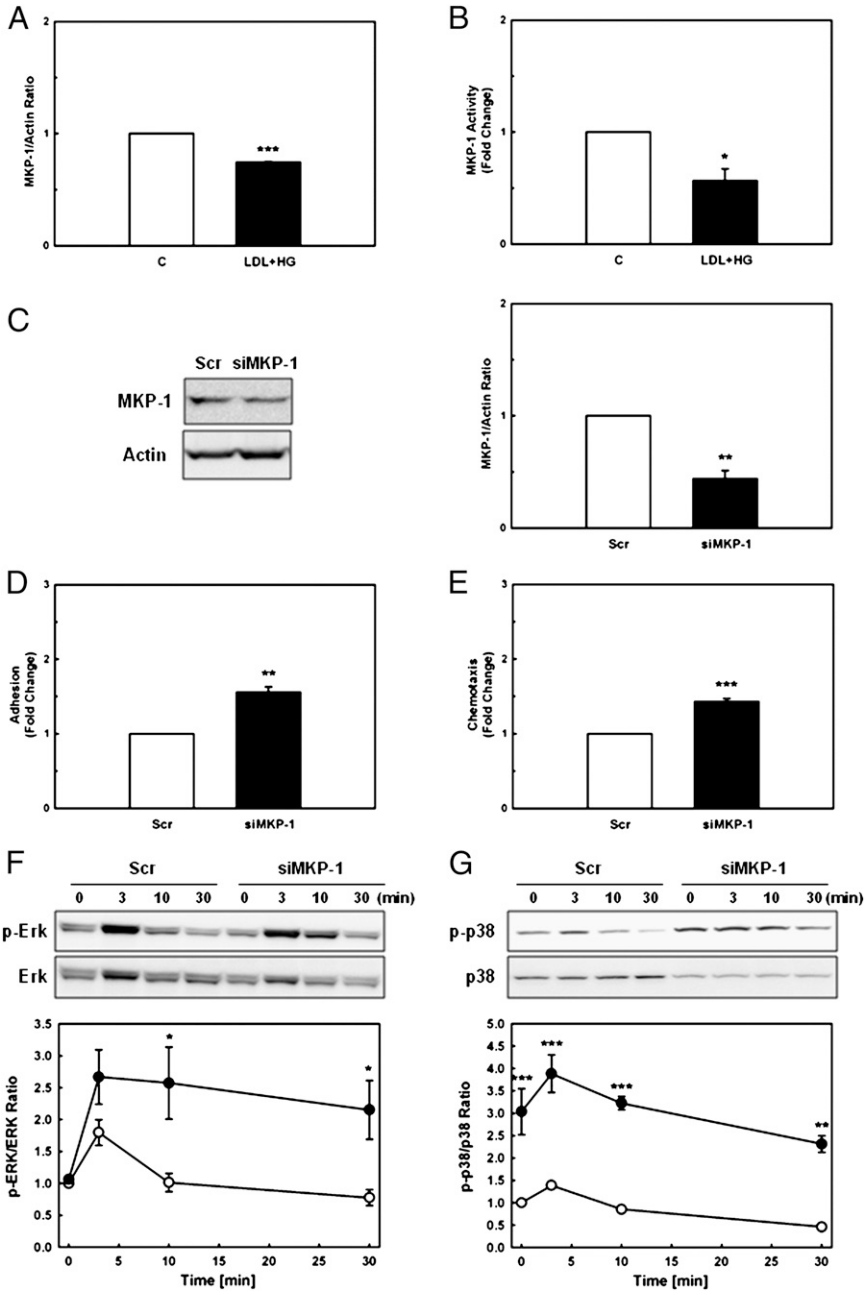

Fig. 2. Metabolic priming decreases both MKP-1 protein levels and phosphatase activity in monocytes. (*A* and *B*) THP-1 monocytes were metabolically primed for 24 h with 100 μg/mL of LDL and 25 mM glucose (LDL+HG) or were preincubated with vehicle (C). MKP-1 protein levels were monitored by Western blot analysis (*A*), and MKP-1 phosphatase activity (*B*) was assessed using a modification of the commercially available Malachite Green-based PTP assay as described in *Materials and Methods*. (*C*–*E*) To assess the effects of MKP-1 deficiency on monocytes, THP-1 monocytes were transfected for 48 h with either nontargeting siRNA (Scr) or siRNA directed against MKP-1 (siMKP-1) and were assayed for cell adhesion (*D*) and chemotaxis (*E*) induced by MCP-1 (2 nM). (*F* and *G*) (*Lower*) MAPK activation by MCP-1 was assessed by Western blot analysis at the indicated times in THP-1 monocytes transfected with either nontargeting siRNA (Scr; open circles) or siRNA directed against MKP-1 (siMKP-1; closed circles) as phosphorylation of ERK (*F*) and p38 (*G*). (*Upper*) Representative Western blots are presented. Results shown are means ± SE of three to five independent experiments. $*P < 0.05$, $**P < 0.01$, $***P < 0.001$ versus vehicle (C) or THP-1 monocytes transfected with scrambled siRNA (Scr), respectively.

tagged MKP-1 in THP-1 monocytes (Fig. S2) and measured ERK and p38 MAPK activation in response to MCP-1. Even before MCP-1 stimulation, ERK activation was damped severely in monocytes overexpressing MKP-1 (Fig. 3*A*). Phosphorylation of p38 was not affected, however (Fig. 3*B*). Both ERK and p38 phosphorylation induced by MCP-1 were suppressed completely in monocytes overexpressing Flag-tagged MKP-1 (Fig. 3 *A* and *B*), and the blunted activation of both ERK and p38 translated into a 47% reduction in monocyte adhesion (Fig. 3*C*) and a 72% inhibition of monocyte chemotaxis in response to MCP-1 (Fig. 3*D*). These results further point to MKP-1 as a central regulator of monocyte adhesion and migration.

Metabolic Stress Promotes *S*-Glutathionylation and Subsequent Proteasomal Degradation of MKP-1. MKPs are sensitive to inactivation via the reversible oxidation of their active-site cysteine (32). We showed that in monocytes metabolic stress promotes protein *S*-glutathionylation, i.e., the formation of mixed disulfides between GSH and reactive protein thiols (17, 18); however, *S*-glutathionylation of MKPs had not been reported. To identify the mechanism by which metabolic stress promotes the inactivation and loss of MKP-1 in monocytes and to explore whether MKP-1 is *S*-glutathionylated in metabolically primed monocytes, we preloaded THP-1 monocytes with biotin-labeled glutathione and performed streptavidin-bead pulldown experiments. Western blot analysis of the biotin-labeled proteins isolated from control monocytes and probed with antibodies directed against MKP-1 revealed a faint band (Fig. 4*A*), indicating that in unprimed monocytes a fraction of MKP-1 already is *S*-glutathionylated. Biotin-labeled MKP-1 levels increased in response to metabolic stress, but only by 26%, an unexpectedly modest increase. However, when THP-1 monocytes were exposed to metabolic stress in the presence of the proteasomal inhibitor MG132, we observed an eightfold increase in MKP-1 *S*-glutathionylation, suggesting that *S*-gluta-

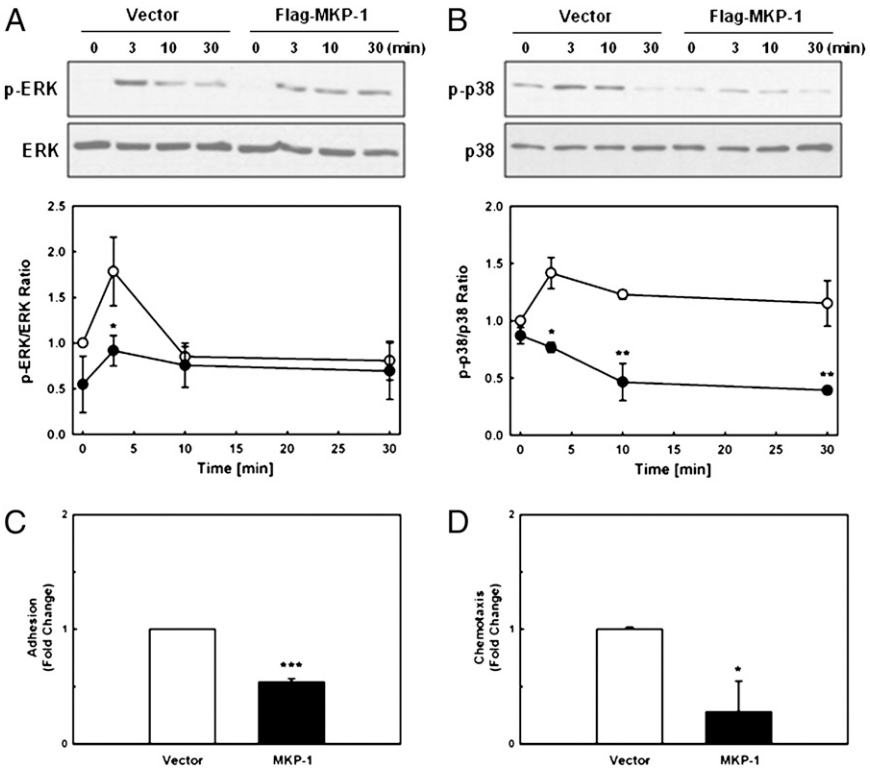

Fig. 3. Overexpression of MKP-1 inhibits activation of Erk and p38 as well monocyte adhesion and chemotaxis induced by MCP-1. (*A* and *B*) (*Lower*) THP-1 monocytes were transfected for 24 h with empty vector pcDNA3.1 (Vector, open circles) or Flag-tagged MKP-1 (closed circles) and were stimulated with 2 nM MCP-1 for the indicated times. ERK phosphorylation (*A*) and p38 phosphorylation (*B*) were assessed by Western blot analysis. (*Upper*) Representative Western blots are shown. (*C* and *D*) Monocyte adhesion (*C*) and chemotaxis (*D*) were assessed in vector-transfected (open bars; Vector) and Flag-MKP-1–overexpressing THP-1 monocytes (closed bars; MKP-1). Results shown are means ± SE of four or five independent experiments. $*P < 0.05$; $***P < 0.001$ versus control vector-transfected THP-1 monocytes, respectively.

thionylation may target MKP-1 for proteasomal degradation. In vitro *S*-glutathionylation of recombinant MKP-1 resulted in a 63% reduction of MKP-1's phosphatase activity, demonstrating that *S*-glutathionylation is sufficient to inactivate MKP-1 and by itself may account for the loss of MKP-1 activity in primed monocytes. To identify the cysteine residues in MKP-1 targeted by *S*-glutathionylation and responsible for the inactivation of the enzyme, we mutated to a serine residue the cysteine residue 258 that is located in the active-site motif and is essential for catalytic activity (33). In contrast to recombinant MKP-1, the C258S mutant of MKP-1 was completely resistant to *S*-glutathionylation (Fig. 4*C* and Fig. S3), suggesting that Cys258 is the only cysteine residue in MKP-1 that is *S*-glutathionylated in response to metabolic stress.

These findings confirm that MKP-1 is *S*-glutathionylated in primed monocytes and suggest that this oxidative modification not only inactivates MKP-1 but also targets the phosphatase for proteasomal degradation. To support this hypothesis further, we also examined whether overexpression of Grx1, the enzyme responsible for the reduction of GSH protein–thiol mixed disulfides, protects both MKP-1 from degradation and metabolically primed monocytes from dysregulated cell adhesion and migration. To this end, THP-1 monocytes were infected with a doxycycline (Dox)-inducible adenoviral construct carrying the sequence for a Grx1-EGFP fusion protein. As shown in Fig. 5*A*, induction of human Grx1 completely prevented the loss of MKP-1 in metabolically primed monocytes. In fact, under these conditions MKP-1 levels exceeded even those found in unprimed control cells, indicating that (*i*) metabolic stress may lead to a mild induction of MKP-1 expression, and (*ii*) that the 25% reduction in MKP-1 levels observed in primed monocytes (Fig. 5*A* and Fig. S4) therefore may be an underestimation of total MKP-1 degradation triggered by metabolic stress. Increasing Grx1 activity also protected monocytes from converting into the hyperadhesive (Fig. 5*B*) and hypermigratory (Fig. 5*C*) phenotype induced by metabolic stress, suggesting that MKP-1 *S*-glutathionylation is essential and mediates monocyte primings by metabolic stress. Thus, S-glutathionylation of MKP-1 not only regulates ERK and p38 activity by inactivating MKP-1 and targeting MKP-1 for proteasomal degradation, but controls monocyte adhesion and migration.

Nox4 Mediates MKP-1 Inactivation Induced by Metabolic Stress. Metabolic stress in monocytes induces Nox4 (17), an inducible NADPH oxidase (Nox) family member we identified in monocytes and macrophages (19), and thereby promotes the *S*-glutathionylation of actin (17). To examine whether Nox4-derived ROS also mediate the *S*-glutathionylation, inactivation, and degradation of MKP-1, THP-1 monocytes were transfected with siRNA directed against Nox4 and then were exposed to metabolic stress, i.e., LDL plus high glucose. As shown in Fig. 6*A*, knockdown of Nox4 completely protected THP-1 monocytes from metabolic stress-induced inactivation of MKP-1. To determine whether induction of Nox4 is sufficient to promote the inactivation and degradation of MKP-1, we overexpressed human Nox4 in THP-1 monocytes using our Dox-inducible adenoviral vector. A 1.8-fold increase in Nox4 (Fig. S5) resulted in a 35% reduction in MKP-1 protein levels (Fig. 6*B*) and a concomitant 45% reduction in MKP-1 activity in these cells (Fig. 6*C*). These findings confirm that Nox4 is required for and mediates the *S*-glutathionylation, inactivation, and subsequent degradation of MKP-1 induced by metabolic stress.

Monocytes from Diabetic *db/db* Mice Show Reduced MKP-1 Activity. Because siRNA-mediated knockdown of MKP-1 in monocytes mimicked the effects of metabolic stress on monocyte adhesion and migration, we next examined whether MKP-1 activity is impaired in the monocytes of mice suffering from metabolic disorders. To this end, we isolated and purified blood monocytes from *db/db* mice, a murine model of type 2 diabetes, and from nondiabetic *db/m* littermates (Table S1). As shown in Fig. 7*A*, MKP-1 activity was 55% lower in monocytes isolated from diabetic *db/db* mice than in monocytes from nondiabetic *db/m* mice. This finding suggests that in mice metabolic stress is associated with a loss of MKP-1 activity in monocytes.

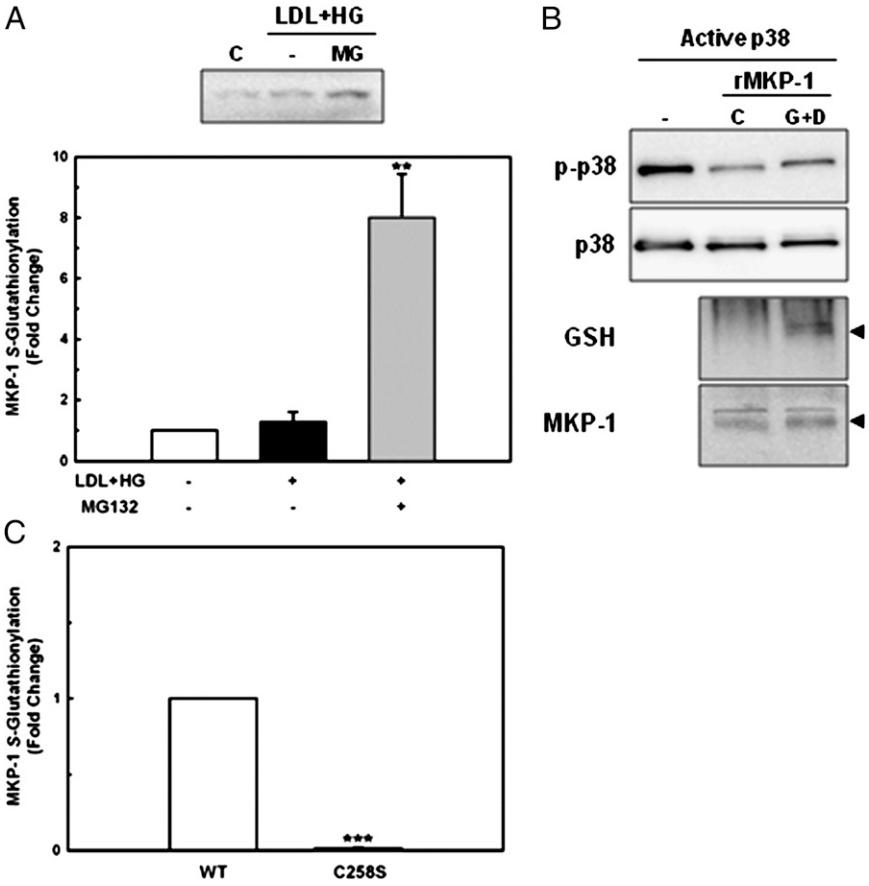

Fig. 4. MKP-1 *S*-glutathionylation on cysteine residue 258 inactivates phosphatase activity and promotes proteasomal degradation. (*A*) (*Lower*) THP-1 monocytes were preincubated with BioGEE (250 μM) and subsequently were primed for 24 h with vehicle (open bar), LDL+HG (black bar), or LDL+HG plus the proteasomal inhibitor MG132 (25 μM) (gray bar). (*Upper*) After precipitation of Biotin-labeled proteins with streptavidin agarose, MKP-1 *S*-glutathionylation was assessed by Western blot analysis using an antibody recognizing MKP-1. $^{**}P < 0.01$. (*B*) (*Lower*) Recombinant MKP-1 was S-glutathionylated in the presence of glutathione (G) and diamide (D). (*Upper*) MKP-1 phosphatase activity was assessed using recombinant phospho-p38 as a substrate, as described in *Materials and Methods*. (*C*) HEK 293T cells were transfected for 24 h with either wild-type Flag-tagged MKP-1 or Flag-tagged MKP-1 in which Cys258 was mutated to a serine residue (C258S) and were subjected to immunoprecipitation with anti-Flag antibodies. To induce *S*-glutathionylation, immunoprecipitated proteins were treated with diamide and GSH as described in *Materials and Methods*. MKP-1 *S*-glutathionylation was assessed by Western blot analysis using antibodies recognizing glutathione and Flag, respectively. Results shown are mean ± SE of three independent experiments. $^{***}P < 0.001$. Representative Western blots are shown in Fig. S3.

Monocytes from MKP-1–Deficient Mice Show Increased Adhesion to Activated Endothelium. Because siRNA-mediated knockdown of MKP-1 in monocytes mimicked the effects of metabolic stress on monocyte adhesion and migration, and because MKP-1 activity is impaired in monocytes of mice suffering from metabolic disorders, we then examined if loss of MKP-1 activity in the blood monocytes of healthy mice would be sufficient to recapitulate monocyte priming and convert monocytes into a proatherogenic phenotype. To test this hypothesis, we purified blood monocytes from wild-type and MKP-1–deficient mice and determined their propensity to adhere to activated primary murine aortic endothelial cells (MAEC) under flow conditions. We observed no significant cell adhesion to unstimulated endothelium by either wild-type or MKP-1–deficient monocytes. Activation of the endothelial layer with TNF-α triggered the adhesion of monocyte from both groups of mice, but the number of adherent cells was 4.8-fold higher when monocytes from MKP-1–null instead of wild-type mice were allowed to flow over the activated endothelium (Fig. 7*B*). These results support a major role for MKP-1 in regulating monocyte adhesion and show that MKP-1 deficiency is sufficient to prime blood monocytes for a dramatically enhanced response to (patho)physiological adhesion cues.

Hematopoietic MKP-1 Deficiency Amplifies Monocyte Priming and Hyperresponsiveness to MCP-1 and Accelerates Atherosclerosis. In atherosclerosis-prone LDL-Real (LDL-R)–null mice, moderate metabolic stress primes blood monocytes and increases their responsiveness to MCP-1–induced recruitment, a phenotypic transformation that is enhanced dramatically if these mice are rendered diabetic (18). Diabetic conditions accelerated the formation of atherosclerotic lesions (18) and were associated with the partial loss of MKP-1 activity in blood monocytes (Fig. 7*A*). We therefore examined whether total MKP-1 deficiency in monocytes in atherosclerosis-prone mice exacerbates the priming effects of metabolic stress on monocytes and if any further sensitization of monocytes to chemoattractants would be sufficient to accelerate atherosclerosis. To this end, we performed bone marrow transplantation experiments in LDL-R–null mice using MKP-1–null and wild-type control mice as bone marrow donors. We induced moderate metabolic stress by feeding the transplant-recipient mice a high-fat diet for 10 wk. Three days before the animals were killed, we assessed monocyte chemotaxis and recruitment in each mouse by implanting s.c. MCP-1–loaded Matrigel plugs (18). As depicted in Fig. 7*C*, mice with monocytes lacking MKP-1 showed a 4.7-fold increase in monocyte responses to MCP-1 chemotaxis, demonstrating that MKP-1 plays a critical role in the regulation of monocyte extravasation and recruitment in vivo. Importantly, the size of atherosclerotic lesions increased 2.6-fold in mice with hematopoietic MKP-1 deficiency compared with mice that received wild-type bone marrow (Fig. 7*D*), confirming that that monocyte responsiveness to chemoattractants is a major determinant of atherogenesis. Plasma total cholesterol and triglyceride levels were identical in the two groups (Table S2) and thus do not account for the acceleration of atherosclerosis in mice with hematopoietic MKP-1 deficiency.

Discussion

In patients with diabetes, the risk for cardiovascular diseases and atherosclerosis increases nearly threefold (34). Despite significant progress in treating diabetic complications, the mechanisms underlying accelerated atherosclerosis associated with diabetes are not fully understood. We have uncovered a thiol redox-sensitive mechanism in monocytes that, upon dysregulation by

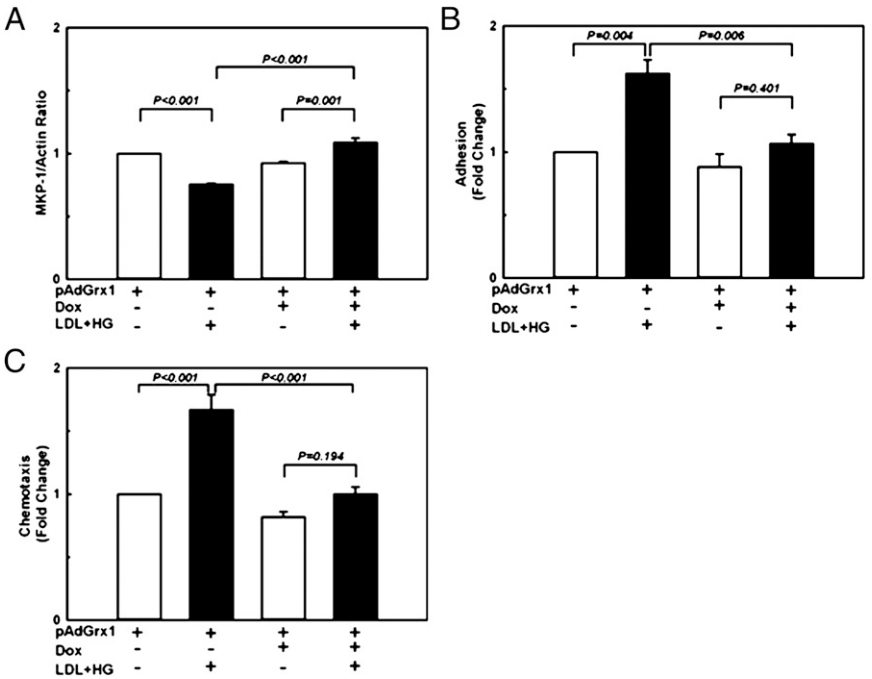

Fig. 5. Overexpression of Grx1 protects against MKP-1 degradation, increased adhesion, and accelerated chemotaxis induced by metabolic stress. THP-1 monocytes were infected with a Dox-inducible adenoviral vector carrying the sequence for a Grx1-EGFP fusion protein (pAdGrx1), and Grx1 expression was induced by treating cells for 24 h with 1 μg/mL Dox. THP-1 monocytes then were treated for 24 h with vehicle or were primed with LDL+HG, and MKP-1 levels (*A*), MCP-1-induced adhesion (*B*), and chemotaxis (*C*) were measured. Results shown are mean ± SE of three independent experiments.

metabolic disorders, primes and transforms monocytes into a hyperchemotactic proatherogenic phenotype, directly linking oxidative stress associated with diabetes to atherogenesis. We showed that in mice the chemotactic activity of monocytes increases with rising levels of hyperglycemia and hyperlipidemia and is associated with increased macrophage recruitment and accelerated atherosclerotic lesion formation (18). We further demonstrated that metabolic stress induces the expression of Nox4, an inducible Nox family member that we identified in monocytes and macrophages (19) and which plays a critical role in monocyte priming by metabolic stress (17). The aim of this study was to elucidate the mechanisms underlying the conversion of monocytes into this hypermigratory, proatherogenic phenotype induced by metabolic stress and to identify the redox-sensitive pathways targeted by Nox4-derived ROS in primed monocytes. Here we show that in primed monocytes, both ERK and p38, the two principal MAPK pathways mediating MCP-1–induced monocyte adhesions and migration (20, 35), become hyperactivated in response to MCP-1 stimulation. Furthermore, activity of MKP-1, a dual-specificity phosphatase involved in the counterregulation of ERK and p38 activation (23), was inhibited significantly in metabolically primed THP-1 monocytes. Importantly, blood monocytes isolated from diabetic mice also showed reduced MKP-1 activity, suggesting that MKP-1 is a target of Nox4-derived ROS induced by diabetic conditions. Indeed, knockdown of MKP-1 in THP-1 monocytes mimicked the effects of metabolic stress, because it resulted in exaggerated MAPK activation in response to MCP-1, increased monocyte adhesion, and accelerated chemotaxis. The critical role of MKP-1 in monocyte priming and dysfunction is supported further by our bone marrow transplantation studies, which show that MKP-1 deficiency in monocytes not only mimics the priming effects of metabolic stress but also dramatically accelerates atherosclerosis in dyslipidemic mice. Therefore it is reasonable to speculate that loss off MKP-1 activity in monocytes also may contribute to accelerated atherosclerosis observed in diabetic patients.

The Nox4-knockdown and -overexpression experiments confirmed that in primed monocytes the inactivation and degradation of MKP-1 is mediated by Nox4-derived H_2O_2. Notably, in unstressed monocytes, Nox4 knockdown had little effect on MKP-1 activity. This result may explain our previous finding that knockdown of Nox4 prevented metabolically stressed monocytes from converting into the hypermigratory phenotype but did not inhibit MCP-1–induced chemotaxis in unprimed cells (17). One potential explanation for this finding may be that monocyte priming requires not only Nox4 protein production but also the transport of Nox4 to its redox-sensitive target. To overcome the slow reaction rate of H_2O_2-mediated thiol oxidation, which we proposed would precede *S*-glutathionylation in cells (17), and to ensure signal specificity, micromolar H_2O_2 concentrations would have to be generated in close proximity to the redox-sensitive target (36). Recent studies by Chen et al. (37) support this concept and highlight the importance of Nox4 localization for the specificity of ROS-mediated signal transduction.

Our data from the MKP-1–knockdown studies demonstrate that partial loss of MKP-1 activity is sufficient to promote monocyte priming and dysfunction. Furthermore, monocytes from MKP-1–null mice show increased cell-adhesion responses, confirming our findings with metabolically primed THP-1 monocytes. However, even though MKP-1 knockdown decreases MKP-1 levels in THP-1 monocytes to significantly lower levels than those observed in metabolically primed THP-1 monocytes (74% versus 44%), the priming effect of MKP-1 knockdown on monocyte adhesion (1.5-fold) and chemotaxis (1.4-fold) was significantly milder than that observed in THP-1 monocytes primed by metabolic stress (i.e., 2.4-fold and 1.8-fold, respectively). Thus, although MKP-1 deficiency is sufficient to promote monocyte priming and clearly is a major contributor to metabolic stress-induced monocyte priming, it is unlikely that *S*-glutathionylation, inactivation, and subsequent degradation of MKP-1 is the sole mechanism contributing to the conversion of blood monocytes into this hyperresponsive, proatherogenic phenotype. In fact, we previously showed that meta-

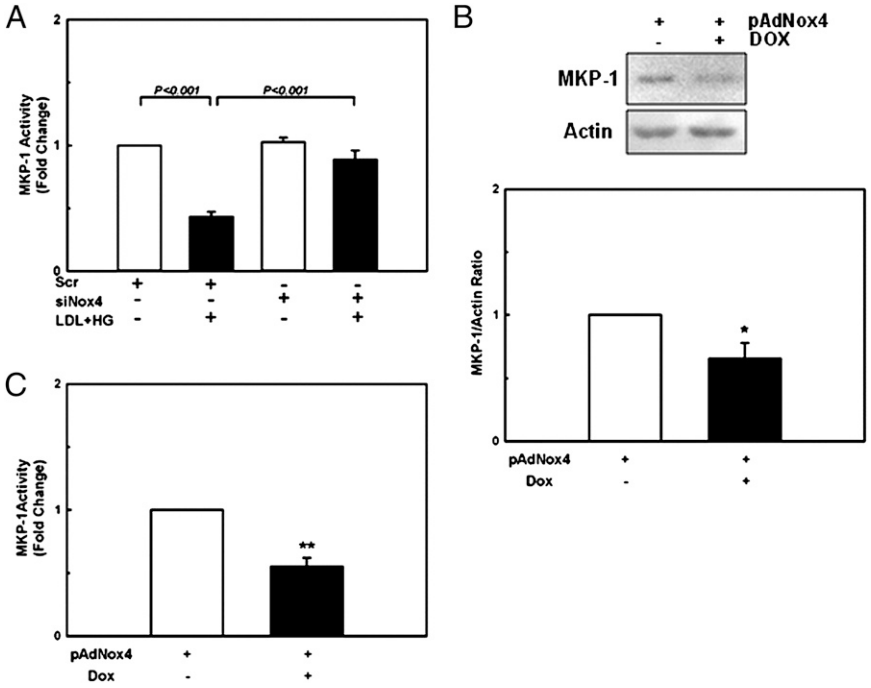

Fig. 6. MKP-1 activity in monocytes is regulated by Nox4. (*A*) Knockdown of Nox4 protects monocytes against metabolic stress-induced inactivation of MKP-1. THP-1 monocytes were transfected for 24 h with Nox4-specific siRNA (siNox4) or nontargeting siRNA (Scr). After siRNA treatment, cells were treated for 24 h with vehicle or were primed with LDL+HG before MKP-1 phosphatase activity was measured in cell lysates. (*B* and *C*) Nox4 overexpression in monocytes decreases MKP-1 protein level and inhibits MKP-1 phosphatase activity. THP-1 monocytes were infected with an inducible adenoviral vector carrying human Nox4. Nox4 expression was induced by adding DOX (1 μg/mL) for 24 h. MKP-1 protein level and phosphatase activity were determined as described in *Materials and Methods*. Results shown are mean ± SE of three independent experiments. $*P < 0.05$, $**P < 0.01$.

bolic stress also promotes *S*-glutathionylation of actin and increases actin turnover, which is likely to contribute to the hyperchemotactic monocyte phenotype induced by metabolic priming (17). At this point it is not clear whether loss of MKP-1 activity and increased actin remodeling are independent or sequential events in the process of monocyte priming. However, both mechanisms clearly require Nox4 induction and are mediated by the targeted and site-specific protein *S*-glutathionylation.

MKPs have an active-site motif very similar to that of protein tyrosine phosphatases (PTPs) (23) and, like PTPs, are sensitive to inactivation via the oxidation of their active-site cysteine (32). PTP-1B was one of the first enzymes whose activity was shown to be regulated by the reversible *S*-glutathionylation of its active-site cysteine, Cys215 (38). Overexpression of Grx1 protected metabolically primed monocytes against the hyperresponsiveness to MCP-1 and prevented the loss MKP-1 protein, suggesting to us that *S*-glutathionylation induced by chronic metabolic stress mediates the loss of MKP-1 activity. Indeed, our studies confirmed that MKP-1 is *S*-glutathionylated in primed monocytes and strongly suggest that MKP-1 *S*-glutathionylation targets the phosphatase to proteasomal degradation. A similar mechanism has been reported for the degradation of γC-crystallin (39). Using recombinant MKP-1, we confirmed that *S*-glutathionylation induced in vitro dramatically reduces the enzyme's activity, demonstrating that thiol oxidation, not protein degradation, is the likely primary mechanism responsible for the loss of MKP-1 activity in both metabolically stressed THP-1 monocytes and blood monocytes isolated from diabetic mice.

DiCorletto and colleagues (40) reported that complete MKP-1 deficiency in apolipoprotein E-null (apoE$^{-/-}$) mice is atheroprotective but only in the aortic sinus and only in female mice. It is possible that the partial atheroprotective properties of complete MKP-1 deficiency reported in apoE$^{-/-}$ mice are related specifically to apoE deficiency or to a unique feature of MKP-1 in the aortic arch of female apoE$^{-/-}$ mice. A more likely explanation supported by our findings is that MKP-1 plays different roles in different cell types, and although MKP-1 deficiency in vascular cells may protect against the formation of atherosclerotic lesions, loss of MKP-1 activity in monocytes actually promotes atherogenesis.

This conclusion is supported by our finding that the MKP-1 deficiency restricted to hematopoietic cells in LDL-R$^{-/-}$ mice not only mirrors the effects of dyslipidemia and diabetes on monocyte priming and macrophage recruitment that we reported previously in this mouse model (18) but also accelerates atherogenesis dramatically. The proatherogenic properties of MKP-1–deficient blood monocytes (Fig. 7*B*) provide further evidence for an atheroprotective role of MKP-1 in monocytes, perhaps explaining the limited atheroprotective effects of complete MKP-1 deficiency reported in the apoE$^{-/-}$ model (40).

A large body of data links oxidative processes or "oxidative stress" induced by metabolic disorders to atherogenesis. However, direct evidence for a causal role of oxidative stress in the development of atherosclerosis is difficult to find (41). With our observation that chronic metabolic stress primes monocytes in a thiol redox-mediated process for dramatically enhanced responsiveness to chemoattractants and increased monocyte recruitment (17, 18), we identified a mechanism by which metabolic disorders may promote atherosclerosis. Our data point to a critical role for MKP-1 in the dysregulation of monocyte adhesion and chemotaxis by metabolic stress and suggest that MKP-1 in monocytes represents a critical mechanistic link between metabolic disorders, including diabetes, and the formation of atherosclerotic lesions.

Materials and Methods

Chemicals and Reagents. *N*-Ethylmaleimide, sodium orthovanadate, sodium fluoride, sanguinarine chloride hydrate, MG132, L-glutathione reduced, and diamide were obtained from Sigma. Biotinylated glutathione ethyl ester (BioGEE) and streptavidin-agarose were purchased from Invitrogen. Com-

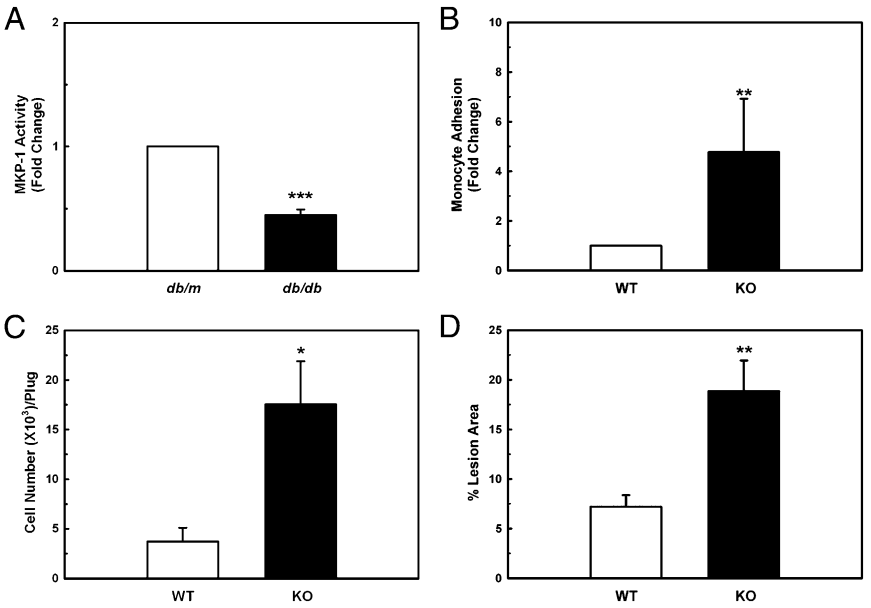

Fig. 7. Loss of monocyte MKP-1 activity increases monocyte adhesion and chemotaxis and promotes atherosclerosis. (*A*) MKP-1 activity is reduced in monocytes from diabetic mice. Blood monocytes were isolated and purified from diabetic (db/db) mice and nondiabetic (db/m) littermates, and MKP-1 phosphatase activity was determined in cell lysates as described in *Materials and Methods*. Results are shown as mean ± SE ($n = 3$). (*B*) Monocytes from MKP-1–deficient (KO) mice show increased adhesion to activated endothelium. Monocytes were isolated from wild-type and MKP-1 KO mice, purified, fluorescently labeled, and allowed to flow over a monolayer of TNF-α–activated murine aortic endothelial cells. The flow chambers were rinsed and digitally photographed, and fluorescent cells were counted. Results are reported as the fold difference in adhered (fluorescent) monocytes between the two groups and are shown as the mean ± SE from five independent experiments. (*C* and *D*) Hematopoietic MKP-1 deficiency increases monocyte chemotaxis and macrophage recruitment into MCP-1–loaded Matrigel plugs and exacerbates atherosclerosis. Bone marrow transplantation was performed in LDL-R–null mice using wild-type and MKP-1–null (KO) mice as bone marrow donors. (*C*) After 10 wk on a high-fat diet, Matrigel supplemented with either vehicle or MCP-1 (500 ng/mL) was injected into the left and right flanks, respectively, of bone marrow recipients. After 3 d, Matrigel plugs were removed surgically and dissolved, and macrophage content was determined in a fluorescence-based cell counter. Results were calculated for each mouse as the difference in macrophage numbers in MCP-1– and vehicle-loaded plugs. (*D*) Aortas of bone marrow recipients were removed, and the size of atherosclerotic lesions was determined by *en face* analysis. Results are shown as mean ± SE ($n = 5$). $^*P < 0.05$, $^{**}P < 0.01$, $^{***}P < 0.001$.

plete, Mini, EDTA-free Protease Inhibitor Mixture Tablets were obtained from Roche Diagnostics. Active p38 was from Abcam. Protein G Sepharose was from GE Healthcare. Antibodies directed against phospho-ERK, total ERK, phospho-p38, and total p38 were purchased from Cell Signaling. Antibodies directed against MKP-1 and actin were from Santa Cruz Biotechnologies, and anti-Flag antibodies were from Sigma.

Animals. MKP-1 wild-type and KO mice were kindly provided by Yusen Liu (The Research Institute at Nationwide Children's Hospital, Columbus, OH) (42). Female LDL-R$^{-/-}$ mice (B6.129S7-Ldlr^{tm1Her}/J) were obtained from Jackson Laboratories. Mice were housed in colony cages, maintained on a 12-h light/12-h dark cycle. Ten 18-wk-old LDL-R$^{-/-}$ mice mice were randomized into two groups and subjected to bone marrow transplantation with either wild-type or MKP-1 KO bone marrow cells. To induce hypercholesterolemia, mice were fed a diet supplemented with fat (21% wt/wt) and cholesterol (0.15% wt/wt) (AIN-76A; BioServ) for a total of 10 wk beginning 3 wk after bone marrow transplantation. Body weights and fasted blood glucose levels were monitored every other week and at the end of the study. All studies were performed with the approval of the University of Texas Health Science Center San Antonio (UTHSCSA) Institutional Animal Care and Use Committee.

Bone Marrow Transplantation. Two weeks before irradiation and bone marrow transplantation, recipient LDLR$^{-/-}$ mice were put on acidified water containing sulfamethoxazole (160 ng/mL) and trimethoprim (32 ng/mL) and were maintained on antibiotics for 4 wk. Bone marrow cells were isolated by flushing the femurs and tibias with Iscove's Modified Dulbecco's Medium (Gibco) containing 2% (vol/vol) FBS as described previously (43). Bone marrow cells (2×10^6 cells in 0.2 mL) were injected via the lateral tail vein into lethally irradiated (two equal doses of 4.7 Gy, 3 h apart; Mark I-68 Irradiator; JL Shepherd) recipient mice ($n = 5$ per group). To monitor leukocyte repopulation in the transplant recipients, blood samples (100 μL) were collected from each mouse 4 wk after transplantation, and differential blood cell counts were performed by the Department of Laboratory Animal Resources at UTHSCSA on a VetScan HM II Analyzer (Abaxis).

In Vivo Matrigel Chemotaxis Assay. Three days before the end of the study, each mouse was injected s.c. in the right and left flanks with growth factor-reduced Matrigel (BD Biosciences) supplemented with vehicle or recombinant MCP-1 (500 ng/mL), respectively (17, 18). The plugs were removed surgically when the mice were killed and were dissolved in dispase (BD Biosciences). Cells were stained with calcein/AM (Invitrogen) and were counted automatically on a video-based, fluorescence cell counter (Nexcelom Bioscience); counts were normalized to collected plug volumes of 50 mg.

Analysis of Atherosclerosis. Atherosclerosis was assessed by *en face* analysis of the ascending and descending aorta as described previously (28). Briefly, after mice were killed, the right atrium was removed, and hearts and aortas were perfused with PBS through the left ventricle. Aortas were fixed with 4% paraformaldehyde in PBS, dissected from the proximal ascending aorta to the bifurcation of the iliac artery, and all adventitial fat was removed. For *en face* analysis, aortas were opened longitudinally, pinned flat onto black paper placed over dental wax, and digitally photographed at a fixed magnification. Total aortic area and lesion areas were calculated using ImagePro Plus 6.0 (Media Cybernetics), and results are expressed as the percent of the lesion area of the aortic arch.

Blood Analysis. Mice were fasted overnight, and blood was obtained by cardiac puncture. Plasma cholesterol and triglyceride levels were determined using enzymatic assay kits (Wako Chemicals) (18).

Mouse Monocyte Isolation and Purification. Blood was drawn from the tail vein of MKP-1 wild-type and KO mice. For the MKP-1 activity assay, blood from individual diabetic C57BL/KS-Lep^{db} (*db/db*) mice and nondiabetic littermates (*db/m*) was kindly provided by Balakuntalam Kasinath (UTHSCSA, San Antonio, TX). Blood was treated with red blood cell lysis buffer (Hybri-Max; Sigma), and monocytes were purified by negative selection using an EasySep mouse monocyte enrichment kit (Stem Cell Technologies), according to the manufacturer's instructions.

MAEC. MAEC were obtained from Cell Biologics and were maintained in basal Mouse Endothelial Cell Medium (Cell Biologics) containing heparin, hydrocortisone, L-glutamine, VEGF, and EGF, and endothelial cell growth was supplemented with 10% FBS (Gibco). MAEC were used between passages 3–5. MAEC were dissociated from flasks using trypsin/EDTA (Gibco) and seeded onto μ-Slide VI chambers (ibidi) coated with 0.2% (wt/wt) gelatin (Sigma-Aldrich). MAEC were stimulated for 20 h with either vehicle or 20 ng/mL human TNF-α (R&D Systems).

Adhesion Assay Under Flow Conditions. Monocyte adhesion was assessed in MAEC-coated flow chambers (μ-Slide VI chambers; ibidi) attached to a perfusion system (ibidi). Flow rates were set to maintain a wall shear stress of 15 dyn/cm^2, i.e., within the range of shear stress reported for normotensive patients (15–20 dyn/cm^2) (44). To visualize monocytes adhering to the MAEC monolayer, purified mouse monocytes were labeled at 37 °C for 10 min with the fluorescent dye calcein/AM (5 μM) (Invitrogen) and then were washed, and resuspended in THP-1 medium. Labeled monocytes were homogeneously infused into the system for 10 min at a concentration of 20×10^3 cells/mL. Flow chambers then were flushed carefully to remove nonadherent cells and the endothelial layer was digitally photographed using a MicroFire camera (Olympus) mounted on a Leica DM1000 fluorescence microscope.

In Vitro Chemotaxis Assay. Chemotaxis assays were conducted in 48-well modified Boyden chamber (NeuroProbe) as described previously (17, 45). Briefly, cells were washed and resuspended ($1–2 \times 10^6$/mL) in THP-1 medium with 0.1% FBS. Subsequently, cells were loaded into the upper wells of the Boyden chamber (NeuroProbe). The lower wells contained either vehicle or MCP-1 (R&D Systems). A 5-μm polyvinyl pyrrolidone-free polycarbonate membrane (NeuroProbe) was layered between the upper and lower chambers, and the chamber was incubated for 3 h at 37 °C and 5% CO_2. The membrane was washed, and cells were removed from the upper side of the filter. Transmigrated cells were stained with Diff-Quik Set (Dade Behring) and counted under a light microscope in five separate high-power fields at 400× magnification.

Human Monocyte Isolation and Culture. Mononuclear cells were isolated from blood obtained from healthy donors (South Texas Blood and Tissue Center) as described previously (46). Primary human monocytes were purified further with magnetic beads (Dynabeads; Untouched Human Monocytes; Invitrogen). Human THP-1 monocytic cells (American Type Culture Collection) were cultured in THP-1 medium, i.e. glucose-free RPMI-1640 (HyClone and Cellgro) supplemented with 5 mM D-glucose, 10% FBS (gibco), 2% GlutaMAX (Gibco), 1% sodium pyruvate (Cellgro), 1% penicillin/streptomycin (Cellgro), 1% Hepes, and 0.1% β-2-mercaptoethanol. Cells were maintained at 37 °C in 5% CO_2 and 95% humidity. For all experiments, cells were used before they reached passage 15.

Metabolic stress was induced by incubating THP-1 monocytes for 24 h in THP-1 medium (5 mM D-glucose) supplemented with 100 μg/mL LDL and 20 mM D-glucose. Primary human monocytes were incubated for 24 h in THP-1 medium with 5% human AB serum (Valley Biomedical, Inc.) instead of FBS and supplemented with 300 μg/mL LDL and 20 mM glucose.

Static Adhesion Assay. THP-1 monocytes (5×10^5 per well) were plated for 40 min at 37 °C onto fibronectin (10 μg/mL)-coated plates in the presence of 2 nM MCP-1. After incubation, nonadherent cells were removed by washing with PBS. Cell adhesion was quantified with the PicoGreen dsDNA Quantitation Assay (Invitrogen).

LDL Isolation. LDL was isolated by ultracentrifugation from pooled plasma from healthy blood donors as described previously (47).

MKP-1 Knockdown. MKP-1–specific siRNA (Sigma) or control siRNA (Dharmacon) was transfected into THP-1 cells by electroporation (Gene Pulser II Electroporation System; Bio-Rad). For electroporation, exponentially growing THP-1 cells (1×10^7 cells) were washed twice and resuspended in 0.2 mL of Opti-MEM (Gibco). The cell suspension was mixed with 2 μM of siRNA and transferred to a cuvettete (0.4-cm gap) (BioRad). After electroporation (250 V, 950 μF) was completed, cells were diluted in 20 mL THP-1 medium and cultured for 48 h at 37 °C.

MKP-1 Overexpression. To generate an N-terminal Flag-tagged MKP-1, a DNA fragment containing full-length human MKP-1 coding sequences (bp 1–1,104) was generated by PCR amplification of human MKP-1 cDNA (Open Biosystems) using the forward primer 5′-AAA AAG CTT GGT ACC AAA ATG GAC TAC AAG GAC GAC GAT GAC AAG GTC ATG GAA GTG GGC ACC CTG-3′ and the reverse primer 5′-AAA CTC GAG TCT AGA TCA GCA GCT GGG AGA GGT CG-3′ followed by cloning into HindIII- and XhoI-restricted multiple cloning site (MCS) of pcDNA3.1 (Invitrogen). To generate C258S point mutant of MKP-1, the megaprimer method was used (48). For the C258S mutant megaprimer, the forward primer 5′-AGGGTGTTTGTCCACTCCCAGGCAGGCATTTCCCGG-3′ and the reverse primer of MKP-1 were used. Transient transfection of plasmids into THP-1 cells was achieved with X-tremeGENE DNA Transfection Reagents, according to the manufacturer's protocol (Roche Diagnostics).

Nox4 Knockdown. Human Nox4 siRNA (Dharmacon) or control siRNA was transfected into THP-1 monocytes with GeneSilencer transfection reagent (Genlantis) for 24 h.

Adenovirus-Mediated Expression of Grx1 and Nox4. To overexpress human Grx1 and Nox4, we used a previously described Dox-controlled Tet-On adenoviral system (17). THP-1 monocytes were incubated for 24 h with the adenoviruses in RPMI medium supplemented with 10% FBS. Transgene expression was induced by adding Dox (1 μg/mL; Sigma) for 24 h.

MKP-1 Activity Assays. MKP-1 activity was determined with a modification of the commercially available MalachiteGreen-based PTP assay (Millipore). To assess MKP-1–specific PTP activity, lysates were analyzed in the absence and presence of 40 μM sanguinarine, a specific inhibitor of MKP-1 (49). Sanguinarine-sensitive PTP activity was attributed to MKP-1. Briefly, assays were initiated by adding 10 μL of phosphotyrosine peptide substrate to cell extracts (2 μg protein) diluted in 20 mM Tris·HCl (pH 7.5), 150 mM NaCl, 1% Nonidet P-40 and warmed to 30 °C. The reaction was stopped after 10 min. MKP-1 activity was assayed spectrophotometrically as the amount of inorganic phosphate released using a VersaMax reader (Molecular Devices). Phosphate released by MKP-1 was quantified from a standard curve prepared with known amounts of KH_2PO_4.

Preparation of GST-MKP-1 Protein. GST-MKP-1 fusion protein was prepared by PCR amplification of human MKP-1 cDNA (Open Biosystems) using the forward primer 5′-AAA GGA TCC ATG GTC ATG GAA GTG GGC ACC CTG-3′ and the reverse primer 5′-AAA CTC GAG TCT AGA TCA GCA GCT GGG AGA GGT CG-3′. The PCR product was cloned into the BamHI and XhoI sites of pGEX4T3 (GE Healthcare). GST-MKP-1 was purified using Glutathione-Sepharose affinity columns from the *Escherichia coli* strain BL21 transformed with pGEX4T3-MKP-1.

In Vitro *S*-Glutathionylation of MKP-1 Protein. GST-MKP-1 bound to Glutathione-Sepharose beads or immunoprecipitated Flag-MKP-1 was *S*-glutathionylated by incubating the protein in dissolved in PBS for 1 h at room temperature with 125 μM GSH and 100 μM diamide. After incubation, beads or immunoprecipitates were washed three times with PBS to remove excess reagents.

Western Blot Analysis. Cells were washed with ice-cold PBS and lysed on ice in RIPA lysis buffer [50 mM Tris·HCl (pH 7.5), 150 mM NaCl, 1% Nonidet P-40, 0.1% SDS, 0.5% sodium deoxycholate] supplemented with protease and phosphatase inhibitors. Aliquots with equal amounts of protein were loaded and separated on a 10% SDS/PAGE gel. Proteins were transferred to PVDF membranes (Millipore) and probed using specific antibodies as indicated. Bands were detected by chemiluminescence on a KODAK Image Station 4000MM. To control for sample loading, blots subsequently were stripped and reprobed for total MAPK or actin.

Detection of *S*-Glutathionylated MKP-1. THP-1 monocytes were preincubated for 1 h with culture medium containing 250 μM BioGEE (50) and primed with LDL plus high glucose in the absence or presence of 25 μM MG132. Cells were washed with ice-cold PBS and lysed in a RIPA buffer containing 10 mM *N*-ethylmaleimide to block further thiol oxidation. Lysates (500 μg protein) were incubated for 1 h at 4 °C with streptavidin-conjugated agarose beads. Then beads were rinsed three times with lysis buffer, *S*-glutathionylated proteins were released from the beads with 10 mM DTT and separated by SDS/PAGE, and MKP-1 levels were evaluated by Western blot analysis.

Statistics. Data were analyzed using ANOVA (Stat 12.0; Sigma). Data were tested for use of parametric or nonparametric post hoc analysis, and multiple comparisons were performed by using the least significant difference method. All data are presented as mean ± SE. Results were considered statistically significant at the $P < 0.05$ level.

ACKNOWLEDGMENTS. We thank Dr. Balakuntalam Kasinath for providing the blood samples from the db/db mice; Dr. Sang-Woo Kim for the pcDNA3.1 vector; Dr. Robert Kramer for permission to use the MKP-1–deficient mice; and Dr. Yusen Liu for providing the mice. This work was supported by Grant HL-70963 from the National Institutes of Health (to R.A.) and by Grant

0855011F (to R.A.) and a Predoctoral Fellowship (10PRE3460002 to C.F.L.) from the American Heart Association, Southwest Affiliate. The Core Optical Imaging Facility is supported by funds from University of Texas Health Science Center at San Antonio (UTHSCSA) and by National Institutes of Health-National Cancer Institute P30 CA54174 (to the Cancer Therapy and Research Center at UTHSCSA).

1. Wellen KE, Hotamisligil GS (2005) Inflammation, stress, and diabetes. *J Clin Invest* 115: 1111–1119.
2. Zhang L, et al. (2003) Diabetes-induced oxidative stress and low-grade inflammation in porcine coronary arteries. *Circulation* 108:472–478.
3. Li J, Wang JJ, Yu Q, Wang M, Zhang SX (2009) Endoplasmic reticulum stress is implicated in retinal inflammation and diabetic retinopathy. *FEBS Lett* 583: 1521–1527.
4. Mangge H, et al. (2004) Low grade inflammation in juvenile obesity and type 1 diabetes associated with early signs of atherosclerosis. *Exp Clin Endocrinol Diabetes* 112(7):378–382.
5. Saraheimo M, Teppo AM, Forsblom C, Fagerudd J, Groop PH (2003) Diabetic nephropathy is associated with low-grade inflammation in Type 1 diabetic patients. *Diabetologia* 46:1402–1407.
6. Glass CK, Witztum JL (2001) Atherosclerosis. the road ahead. *Cell* 104:503–516.
7. Libby P (2002) Inflammation in atherosclerosis. *Nature* 420:868–874.
8. Cipolletta C, Ryan KE, Hanna EV, Trimble ER (2005) Activation of peripheral blood CD14+ monocytes occurs in diabetes. *Diabetes* 54:2779–2786.
9. Kowala MC, Recce R, Beyer S, Gu C, Valentine M (2000) Characterization of atherosclerosis in LDL receptor knockout mice: Macrophage accumulation correlates with rapid and sustained expression of aortic MCP-1/JE. *Atherosclerosis* 149:323–330.
10. Swirski FK, et al. (2006) Monocyte accumulation in mouse atherogenesis is progressive and proportional to extent of disease. *Proc Natl Acad Sci USA* 103:10340–10345.
11. Li SL, et al. (2006) Enhanced proatherogenic responses in macrophages and vascular smooth muscle cells derived from diabetic db/db mice. *Diabetes* 55:2611–2619.
12. Tacke F, et al. (2007) Monocyte subsets differentially employ CCR2, CCR5, and CX3CR1 to accumulate within atherosclerotic plaques. *J Clin Invest* 117:185–194.
13. Devaraj S, et al. (2006) Increased monocytic activity and biomarkers of inflammation in patients with type 1 diabetes. *Diabetes* 55:774–779.
14. Boring L, Gosling J, Cleary M, Charo IF (1998) Decreased lesion formation in CCR2-/- mice reveals a role for chemokines in the initiation of atherosclerosis. *Nature* 394: 894–897.
15. Gosling J, et al. (1999) MCP-1 deficiency reduces susceptibility to atherosclerosis in mice that overexpress human apolipoprotein B. *J Clin Invest* 103:773–778.
16. Gu L, et al. (1998) Absence of monocyte chemoattractant protein-1 reduces atherosclerosis in low density lipoprotein receptor-deficient mice. *Mol Cell* 2:275–281.
17. Ullevig S, et al. (2012) NADPH oxidase 4 mediates monocyte priming and accelerated chemotaxis induced by metabolic stress. *Arterioscler Thromb Vasc Biol* 32:415–426.
18. Qiao M, et al. (2009) Thiol oxidative stress induced by metabolic disorders amplifies macrophage chemotactic responses and accelerates atherogenesis and kidney injury in LDL receptor-deficient mice. *Arterioscler Thromb Vasc Biol* 29:1779–1786.
19. Lee CF, Qiao M, Schröder K, Zhao Q, Asmis R (2010) Nox4 is a novel inducible source of reactive oxygen species in monocytes and macrophages and mediates oxidized low density lipoprotein-induced macrophage death. *Circ Res* 106:1489–1497.
20. Ashida N, Arai H, Yamasaki M, Kita T (2001) Distinct signaling pathways for MCP-1-dependent integrin activation and chemotaxis. *J Biol Chem* 276:16555–16560.
21. Arefieva TI, Kukhtina NB, Antonova OA, Krasnikova TL (2005) MCP-1-stimulated chemotaxis of monocytic and endothelial cells is dependent on activation of different signaling cascades. *Cytokine* 31:439–446.
22. Owens DM, Keyse SM (2007) Differential regulation of MAP kinase signalling by dual-specificity protein phosphatases. *Oncogene* 26:3203–3213.
23. Patterson KI, Brummer T, O'Brien PM, Daly RJ (2009) Dual-specificity phosphatases: Critical regulators with diverse cellular targets. *Biochem J* 418:475–489.
24. Liu WH, Cheng YC, Chang LS (2009) ROS-mediated p38alpha MAPK activation and ERK inactivation responsible for upregulation of Fas and FasL and autocrine Fas-mediated cell death in Taiwan cobra phospholipase A(2)-treated U937 cells. *J Cell Physiol* 219:642–651.
25. Bhatt NY, et al. (2002) Macrophage-colony-stimulating factor-induced activation of extracellular-regulated kinase involves phosphatidylinositol 3-kinase and reactive oxygen species in human monocytes. *J Immunol* 169:6427–6434.
26. Guyton KZ, Liu Y, Gorospe M, Xu Q, Holbrook NJ (1996) Activation of Mitogen-activated Protein Kinase by HO. *J Biol Chem* 271:4138–4142.
27. Aikawa R, et al. (1997) Oxidative stress activates extracellular signal-regulated kinases through Src and Ras in cultured cardiac myocytes of neonatal rats. *J Clin Invest* 100: 1813–1821.
28. Ogura M, Kitamura M (1998) Oxidant stress incites spreading of macrophages via extracellular signal-regulated kinases and p38 mitogen-activated protein kinase. *J Immunol* 161:3569–3574.
29. Kurata S (2000) Selective activation of p38 MAPK cascade and mitotic arrest caused by low level oxidative stress. *J Biol Chem* 275:23413–23416.
30. Barrett WC, et al. (1999) Regulation of PTP1B via glutathionylation of the active site cysteine 215. *Biochemistry* 38:6699–6705.
31. Jacob A, Smolenski A, Lohmann SM, Begum N (2004) MKP-1 expression and stabilization and cGK Ialpha prevent diabetes- associated abnormalities in VSMC migration. *Am J Physiol Cell Physiol* 287:C1077–C1086.
32. Kamata H, et al. (2005) Reactive oxygen species promote TNFalpha-induced death and sustained JNK activation by inhibiting MAP kinase phosphatases. *Cell* 120: 649–661.
33. Sun H, Charles CH, Lau LF, Tonks NK (1993) MKP-1 (3CH134), an immediate early gene product, is a dual specificity phosphatase that dephosphorylates MAP kinase in vivo. *Cell* 75:487–493.
34. Roger VL, et al. (2011) Heart disease and stroke statistics–2012 update: A REPORT from the American Heart Association. *Circulation* 125:e12–e230.
35. Quehenberger O (2005) Thematic review series: The immune system and atherogenesis. Molecular mechanisms regulating monocyte recruitment in atherosclerosis. *J Lipid Res* 46:1582–1590.
36. Winterbourn CC, Hampton MB (2008) Thiol chemistry and specificity in redox signaling. *Free Radic Biol Med* 45:549–561.
37. Chen K, Kirber MT, Xiao H, Yang Y, Keaney JF, Jr. (2008) Regulation of ROS signal transduction by NADPH oxidase 4 localization. *J Cell Biol* 181:1129–1139.
38. Shelton MD, Chock PB, Mieyal JJ (2005) Glutaredoxin: Role in reversible protein s-glutathionylation and regulation of redox signal transduction and protein translocation. *Antioxid Redox Signal* 7:348–366.
39. Zetterberg M, et al. (2006) Glutathiolation enhances the degradation of gammaC-crystallin in lens and reticulocyte lysates, partially via the ubiquitin-proteasome pathway. *Invest Ophthalmol Vis Sci* 47:3467–3473.
40. Shen J, et al. (2010) Lack of mitogen-activated protein kinase phosphatase-1 protects ApoE-null mice against atherosclerosis. *Circ Res* 106:902–910.
41. Stocker R, Keaney JF, Jr. (2005) New insights on oxidative stress in the artery wall. *J Thromb Haemost* 3:1825–1834.
42. Nelin LD, et al. (2007) MKP-1 switches arginine metabolism from nitric oxide synthase to arginase following endotoxin challenge. *Am J Physiol Cell Physiol* 293:C632–C640.
43. Qiao M, et al. (2007) Increased expression of cytosolic and mitochondrial glutathione reductase in macrophages inhibits atherosclerotic lesion development in LDL receptor-deficient mice. *Arterioscler Thromb Vasc Biol* 27:1375–1382.
44. Davies RJ, Morrell NW (2008) Molecular mechanisms of pulmonary arterial hypertension: Role of mutations in the bone morphogenetic protein type II receptor. *Chest* 134:1271–1277.
45. Ullevig SL, Zhao Q, Zamora D, Asmis R (2011) Ursolic acid protects diabetic mice against monocyte dysfunction and accelerated atherosclerosis. *Atherosclerosis* 219: 409–416.
46. Wintergerst ES, Jelk J, Asmis R (1998) Differential expression of CD14, CD36 and the LDL receptor on human monocyte-derived macrophages. A novel cell culture system to study macrophage differentiation and heterogeneity. *Histochem Cell Biol* 110: 231–241.
47. Wintergerst ES, Jelk J, Rahner C, Asmis R (2000) Apoptosis induced by oxidized low density lipoprotein in human monocyte-derived macrophages involves CD36 and activation of caspase-3. *Eur J Biochem* 267:6050–6059.
48. Sarkar G, Sommer SS (1990) The "megaprimer" method of site-directed mutagenesis. *Biotechniques* 8:404–407.
49. Vogt A, et al. (2005) The benzo[c]phenanthridine alkaloid, sanguinarine, is a selective, cell-active inhibitor of mitogen-activated protein kinase phosphatase-1. *J Biol Chem* 280:19078–19086.
50. Meissner F, Molawi K, Zychlinsky A (2008) Superoxide dismutase 1 regulates caspase-1 and endotoxic shock. *Nat Immunol* 9:866–872.